

Journal Pre-proofs

Antimicrobial and Antitumor Activity of Peptidomimetics Synthesized from Amino Acids

Huan Li, Shuang Fu, Yudan Wang, Xuan Yuan, Lijia Liu, Hongxing Dong, Qiang Wang, Zhijia Zhang

PII: S0045-2068(20)31804-6
DOI: <https://doi.org/10.1016/j.bioorg.2020.104506>
Reference: YBIOO 104506

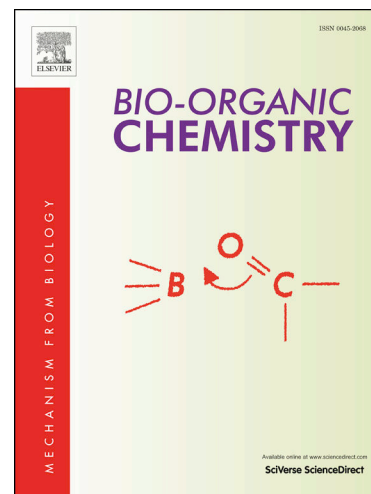
To appear in: *Bioorganic Chemistry*

Received Date: 2 June 2020
Revised Date: 24 September 2020
Accepted Date: 19 November 2020

Please cite this article as: H. Li, S. Fu, Y. Wang, X. Yuan, L. Liu, H. Dong, Q. Wang, Z. Zhang, Antimicrobial and Antitumor Activity of Peptidomimetics Synthesized from Amino Acids, *Bioorganic Chemistry* (2020), doi: <https://doi.org/10.1016/j.bioorg.2020.104506>

This is a PDF file of an article that has undergone enhancements after acceptance, such as the addition of a cover page and metadata, and formatting for readability, but it is not yet the definitive version of record. This version will undergo additional copyediting, typesetting and review before it is published in its final form, but we are providing this version to give early visibility of the article. Please note that, during the production process, errors may be discovered which could affect the content, and all legal disclaimers that apply to the journal pertain.

© 2020 Elsevier Inc. All rights reserved.



Antimicrobial and Antitumor Activity of Peptidomimetics Synthesized from Amino Acids

Huan Li¹, Shuang Fu², Yudan Wang^{1*}, Xuan Yuan¹, Lijia Liu^{1*}, Hongxing Dong¹, Qiang Wang^{1*}, Zhijia Zhang¹

¹Key Laboratory of Superlight Materials & Surface Technology, Ministry of Education, Institute of Advanced Marine Materials, College of Materials Science and Chemical Engineering, Harbin Engineering University, Harbin 150001, China;² College of pharmacy, Qiqihar Medical University, Qiqihar, 161000, China;

Corresponding authors: dqllj2000@163.com (Y. Wang); liulijia@hrbeu.edu.cn (L. Liu)
13864285521@126.com (Q. Wang)

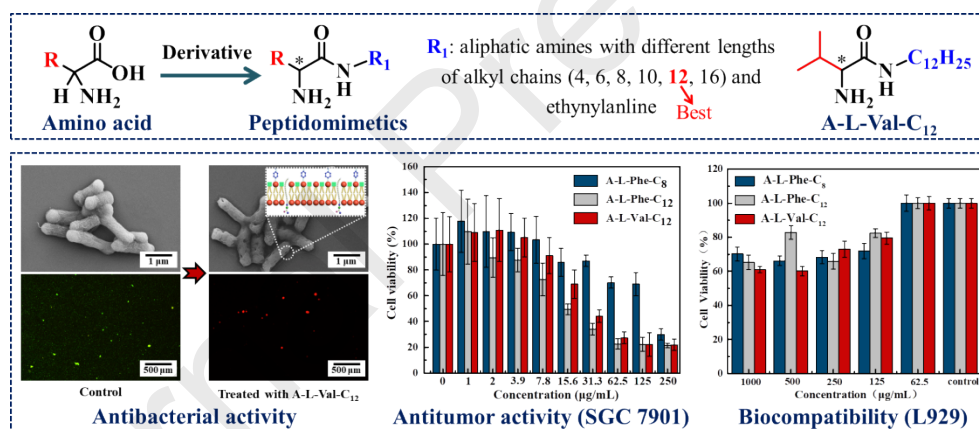
Abstract

Thirteen cationic peptidomimetics derived from amino acids bearing an alkyl or ethynylphenyl moiety that mimic the structure of cationic antibacterial peptides were designed and synthesized using a simple coupling reaction of an amino acid with a substituted amine. Antibacterial activities of the resulting peptidomimetics against drug-sensitive bacteria, such as Gram-positive *Staphylococcus aureus* (*S. aureus*) and *Bacillus subtilis*, Gram-negative *Escherichia coli* (*E. coli*) and *Salmonella enterica*, and a drug-resistant bacterium, methicillin-resistant *S. aureus* (MRSA), were systematically evaluated. Most peptidomimetics show significant broad-spectrum antibacterial activity. A-L-Iso-C₁₂ (isoleucine derivative bearing a dodecyl moiety) show MICs of 2.5 µg/mL against *S. aureus* and 4 µg/mL against MRSA and A-

L-Val-C₁₂ (valine derivative bearing a dodecyl moiety) show MICs of 1.67 µg/mL against *E. coli* and 8.3 µg/mL against MRSA. A-L-Val-C₁₂ showed low cytotoxicity toward L929 cells in comparison with SGC 7901 cells, indicating tumor-directed killing by peptidomimetics while avoiding toxicity to normal cells. The influences of type of amino acid and substituent, length of substituent, and stereochemistry of amino acids on antibacterial activity and cytotoxicity of peptidomimetics were systematically investigated. The results indicate that this series of cationic peptidomimetics derived from amino acids display antitumor activity and may be useful for treatment of bacterial infections.

Keywords: amino acid; antibacterial; antitumor; low cytotoxicity; peptide

Graphical abstract



1. Introduction

Bacterial resistance to antibiotic agents is increasing, making human infections increasingly difficult to treat [1]. Drug-resistant bacteria such as methicillin-resistant *Staphylococcus aureus* (MRSA) [2], *Extended-Spectrum β-lactamase-producing bacteria* (ESBLs) [3, 4], and drug-resistant *Mycobacterium tuberculosis* [5] are now spreading worldwide [6-8]. In addition to clinically excessive use and misuse of antibiotics, bacteria adhere and accumulate on biofilm

formed under appropriate conditions, and attached bacteria can obtain drug resistance genes through horizontal gene transfer [9, 10]. The increase in bacterial resistance to antibiotics and stagnation of research on novel agents has led to an urgent need to develop new antibacterial drugs.

Natural biofilm-active compounds, such as antibacterial peptides (AMPs) and cationic liposomes, and other lipophilic biofilm-active compounds that kill bacteria, fungi, protozoa, viruses, and even cancer cells are considered as antibacterial agents of the future [11-13]. However, limited selectivity, high *in vivo* toxicity, and high manufacturing costs of antibacterial peptides limit their use as clinical antibacterial agents [14]. Synthesis of a variety of peptide mimics to replace natural antibacterial peptides may address these issues [15, 16]. Amino acids have the advantages of good biocompatibility, low toxicity, wide range of sources, and low costs. Derivatives of these compounds can be used for the development of new drugs. Using amino acids to construct amphiphilic molecules that mimic structure and mechanism of antibacterial peptides, new antibacterial peptidomimetics have been developed, such as α -peptide [17], β -peptide [14, 18], oligoyl lysine [8], α -AA peptide [19], cationic liposomes, and cationic amphiphilic compounds [20, 21]. Amino acids in these molecules can recognize the outer membrane of bacteria and can quickly kill bacteria by destroying this membrane. Some new compounds show rapid and effective antibacterial properties against both Gram-positive and Gram-negative bacteria. Bacteria show low resistance to these agents [16, 20].

Peptidomimetics can be used as antimicrobial agents and as carriers for gene therapy and drugs for cancer treatment. As chemotherapeutic substances, cationic liposomes are naturally positively charged or positively charged by protonation at normal physiological pH. These agents electrostatically combine with negatively charged phosphates on the surface of DNA to inhibit DNA formation and growth of tumor cells [22, 23]. Cation and amphiphilic anti-cancer active

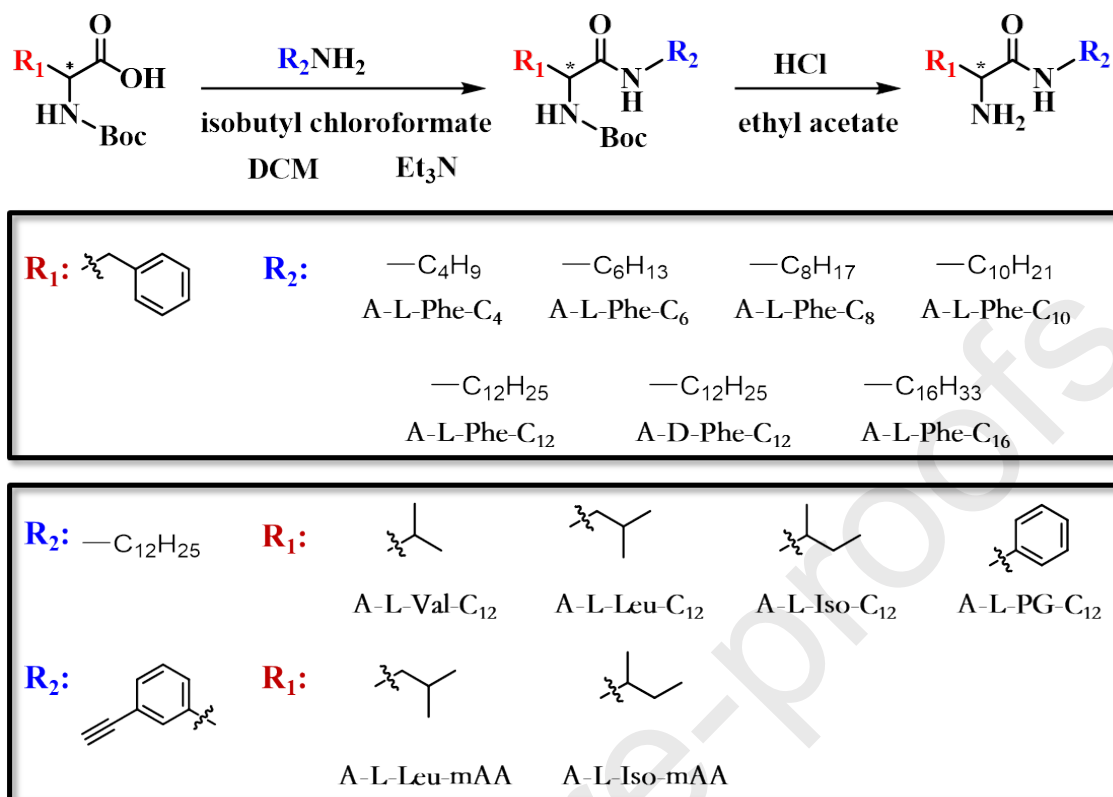
peptides also interact with cancer cells through electrostatic and hydrophobic interactions, leading to cancer cell necrosis or apoptosis [24-29].

A series of cationic antibacterial peptidomimetics with alkyl or phenylethynyl groups were synthesized using amino acids as raw materials. These peptidomimetics exhibit excellent broad-spectrum antibacterial activity and notable killing of SGC 7901 tumor cells. Further, these agents show low cytotoxicity to L929 cells and good biocompatibility. The effects of the type and length of substituent groups and the type and stereo configuration of the amino acid residues on antibacterial properties and cytotoxicity of peptidomimetics were systematically investigated. The mechanism of antibacterial action was also explored.

2. Results and discussion

2.1. Synthesis of the peptidomimetics

Several amino acids were separately reacted with aliphatic amines with different alkyl chain lengths, ranging from 4 to 16 carbon atoms, or with an ethynylaniline to produce thirteen cationic peptidomimetics (Scheme 1). Reaction products were characterized with $^1\text{H-NMR}$, $^{13}\text{C-NMR}$, and FTIR [30].



Scheme 1. Synthesis of the peptidomimetics

2.2. Antibacterial Activity

2.2.1. Minimum inhibitory concentrations (MIC)

Antibacterial efficacy was evaluated by minimum inhibitory concentrations (MIC) of peptidomimetics (Table 1). Peptidomimetics (entries 5, 6, 8-11 in Table 1) show substantial activity against both Gram-positive and Gram-negative bacteria, but a higher activity against the latter. For instance, peptidomimetics with dodecyl chains (entries 5, 6, 8-11 in Table 1) display a range of MIC values against the Gram-positive bacteria of 1 $\mu\text{g/mL}$ - 20 $\mu\text{g/mL}$, compared to MICs of 1.67 $\mu\text{g/mL}$ - 6.5 $\mu\text{g/mL}$ against the Gram-negative bacteria.

The length of alkyl chains is crucial to antibacterial activity. A-L-Phe-C₄, with the shortest aliphatic chain (butyl chain) shows poor antibacterial activity against both Gram-positive *S. aureus*

and Gram-negative *E. coli* MIC values of 1250 and 312 $\mu\text{g/mL}$, respectively. The activity of peptidomimetics is substantially promoted by changing the short butyl chain to a longer octanoyl chain (A-L-Phe-C₈, MIC=39 $\mu\text{g/mL}$ against both *S. aureus* and *E. coli*). Further increase of alkyl chain length led to additional reduction in MIC. For instance, A-L-Phe-C₁₂ with a dodecyl chain shows MIC values of 5 $\mu\text{g/mL}$ and 2.5 $\mu\text{g/mL}$ against *S. aureus* and *E. coli*, respectively. However, any greater chain length resulted in decreased activity, as observed for the A-L-Phe-C₁₆ hexadecanoyl compound, MIC =1250 $\mu\text{g/mL}$ against *E. coli*. A parabolic chain length response curve was thus characteristic for structure–activity relationship (SAR) for peptidomimetics. Optimum lipophilicity lies somewhere between dodecanoyl and hexadecanoyl chain length.

Amino acid residues in peptidomimetics also have an important effect on the antibacterial activity. Peptidomimetics with the same dodecyl chain (entries 5, 7-11 in Table 1) show significant differences in antibacterial activity among in amino acid residues. Peptidomimetics derived from lipophilic amino acids, such as A-L-Val-C₁₂, A-L-Leu-C₁₂, and A-L-Iso-C₁₂ show significant activity, especially against MRSA, MIC=4-8.3 $\mu\text{g/mL}$. MICs of these three mimetics are comparable to the MIC against MRSA of MSI-78, an AMP currently undergoing phase III clinical trials as a topical antibiotic. Antibacterial activity of peptidomimetics based on aromatic amino acids, A-L-Phe-C₁₂, and A-L-PG-C₁₂, is reduced, MIC=15.6-16.6 $\mu\text{g/mL}$. Further, A-L-Leu-mAA with ethynyl aniline and L-leucine residues shows activity against all tested bacteria. Similar MICs were found for A-L-Phe-C₄. Peptidomimetics (entries 12, 13 in Table 1) with the same ethynyl aniline residues derived from different amino acids also display differences in antibacterial activity. The activity of A-L-Iso-mAA with a L-isoleucine residue is lower than that of A-L-Leu-mAA with an L-leucine residue.

The structure-activity relationships peptidomimetics indicate that structure and chain lengths

of hydrophobic moieties and the structure of the base amino acid are important for antibacterial performance. Substantial antibacterial activity of the peptidomimetics against MRSA suggests potential for antibacterial medicine.

Journal Pre-proofs

Table 1. Antibacterial of the peptidomimetics

Entry	Compound	MIC ($\mu\text{g/mL}$)				
		Gram-negative		Gram-positive		Drug resistant bacteria
		<i>E.coli</i>	<i>Salmonella</i>	<i>S.aureus</i>	<i>Bacillus subtilis</i>	MRSA
1	A-L-Phe-C ₄	312	416	1250	416	624
2	A-L-Phe-C ₆	156	156	624	156	312
3	A-L-Phe-C ₈	39	62.5	39	78	52
4	A-L-Phe-C ₁₀	10	15.6	13.3	39	20
5	A-L-Phe-C ₁₂	5	5	2.5	10	16.6
6	A-D-Phe-C ₁₂	5	10	5	8.3	20
7	A-L-Phe-C ₁₆	1250	625	1250	625	1250
8	A-L-Val-C ₁₂	1.67	6.5	3.3	4.2	8.3
9	A-L-Leu-C ₁₂	2.5	4.17	3.3	10	6.25
10	A-L-Iso-C ₁₂	2	5	2.5	5	4
11	A-L-PG-C ₁₂	2.5	3.9	7.8	10	15.6
12	A-L-Leu-mAA	10.6	15.6	10.6	15.6	31.2
13	A-L-Iso-mAA	15.6	15.6	31.2	31.2	62.4
14	LEV ^a	20	- ^b	- ^b	- ^b	- ^b
15	GEN ^c	- ^b	- ^b	2	- ^b	- ^b
16	MSI-78	16-32 ^d	- ^b	8-16 ^d	- ^b	16-32 ^d

^a LEV (levofloxacin).

^b Not determined.

^c GEN (gentamycin).

^d Literature values [33].

2.2.2. Inhibition zone

Inhibition zone tests are used to characterize both the antibacterial activity and permeability of the peptidomimetics concurrently. Inhibition zone experiments of peptidomimetics with both Gram-negative and positive bacteria were conducted (Fig. 1). After a 24 h incubation, inhibition zones were clearly observed for peptidomimetics A-L-Phe-C₈, A-L-Phe-C₁₂, A-L-Iso-C₁₂, A-L-Leu-mAA, and A-L-Iso-mAA against both bacteria types; no significant inhibition zones appeared for peptidomimetics A-L-Phe-C₄, A-L-Phe-C₁₂, A-D-Phe-C₁₂, A-L-Val-C₁₂ (Fig. 1b and 1c). Among peptidomimetics with dodecyl chains, A-L-Iso-C₁₂ derived from isoleucine showed the largest inhibition zone against *S. aureus* and *E. coli*, consistent with its low MIC. A-L-Iso-C₁₂ displays both high antibacterial activity and notable permeability. Testing of aromatic peptidomimetics with different chain lengths (A-L-Phe-C_n, n=4, 6, 8, 10, 12, 16) shows that A-L-Phe-C₈ induced the largest zone of inhibition. Also, peptidomimetics, A-L-Leu-mAA, and A-L-Iso-mAA with ethnyl aniline residues, showed large inhibition zones against both bacteria types (Fig. 1b and 1c). Thus, a combination of antibacterial activity and permeability may result in synergistic antibacterial activity.

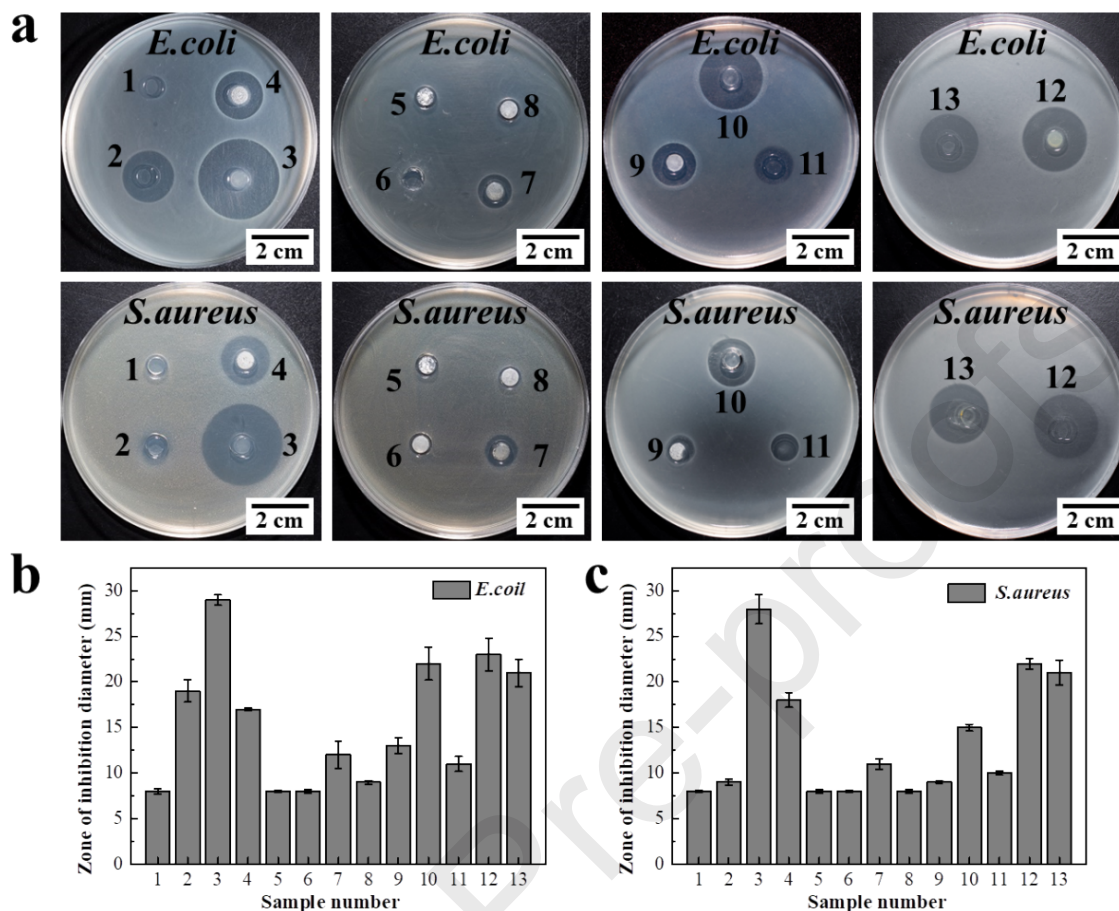


Fig. 1. Antibacterial activity of peptidomimetics: (a) images of punch well agar diffusion test against *E. coli* and *S. aureus*; (b) zone of inhibition diameter against *E. coli*; (c) zone of inhibition diameter against *S. aureus*.

2.3. Inhibition of bacterial growth

Growth rates of bacteria were evaluated using OD_{600} to evaluate inhibition of bacterial growth by the peptidomimetics. Higher OD_{600} indicates higher concentrations of bacteria and poorer antibacterial activity. Compared with controls, concentrations of A-L-Phe- C_{12} less than 2 did not inhibit the growth of *E. coli*. Growth of bacteria was significantly inhibited at a concentration of 5 $\mu\text{g/mL}$ and almost stopped when the concentration increased to 10 $\mu\text{g/mL}$ (Fig. 2a and 2b). A concentration of A-L-Val- C_{12} of 1 $\mu\text{g/mL}$ significantly inhibited *E. coli* growth. At 10 $\mu\text{g/mL}$,

bacteria were dead. Both peptidomimetics exhibited excellent antibacterial activity. A-L-Val-C₁₂ exhibited better antibacterial activity than A-L-Phe-C₁₂, despite identical dodecyl chains. Amino acid residues significantly affect the antibacterial activity of peptidomimetics.

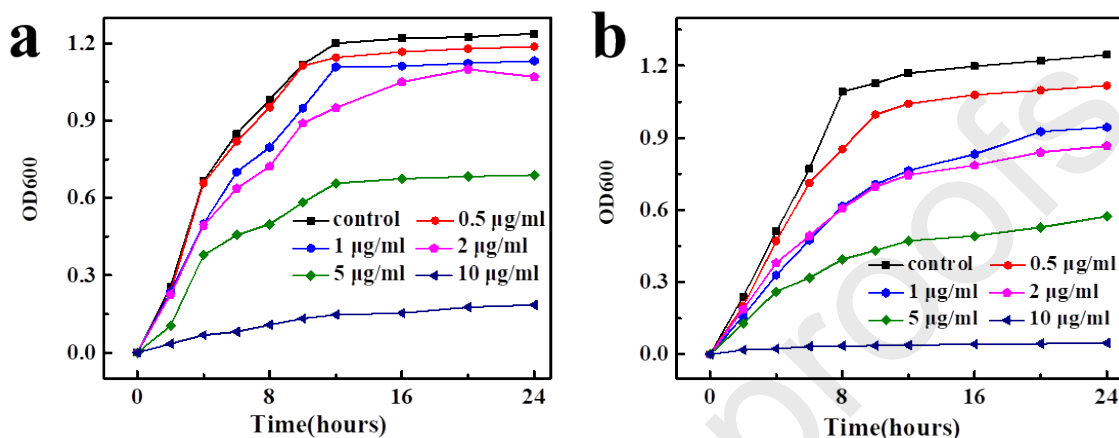


Fig. 2. Bacterial growth curves of *E. coli* treated with peptidomimetics: (a) A-L-Phe-C₁₂; (b) A-L-Val-C₁₂.

2.4. Bactericidal kinetics

Time-kill kinetics of peptidomimetics against *E. coli* provide a rate for bactericidal action. *E. coli* was cultured to stationary phase, then treated with peptidomimetics, A-L-Phe-C₁₂, and A-L-Val-C₁₂, at concentrations of 5 µg/mL, 10 µg/mL, 15 µg/mL and 20 µg/mL. These peptidomimetics show excellent bactericidal activity and rates of bactericidal action increases with increasing concentration. (Fig. 3).

At concentrations below 10 µg/mL of A-L-Phe-C₁₂, the growth of stationary-phase bacteria was inhibited, and bacterial reproduction was slow. When the concentration increased to 20 µg/mL, the bacterial population was significantly reduced, and almost all bacteria were killed after 4 hours (Fig. 3a). A-L-Val-C₁₂ exhibited more rapid biocidal action reducing the bacterial population by $\sim 7 \log_{10}$ (CFU/mL) at a concentration of 20 µg/mL in only 10 min. This treatment killed almost all

stationary-phase bacteria. (Fig. 3b).

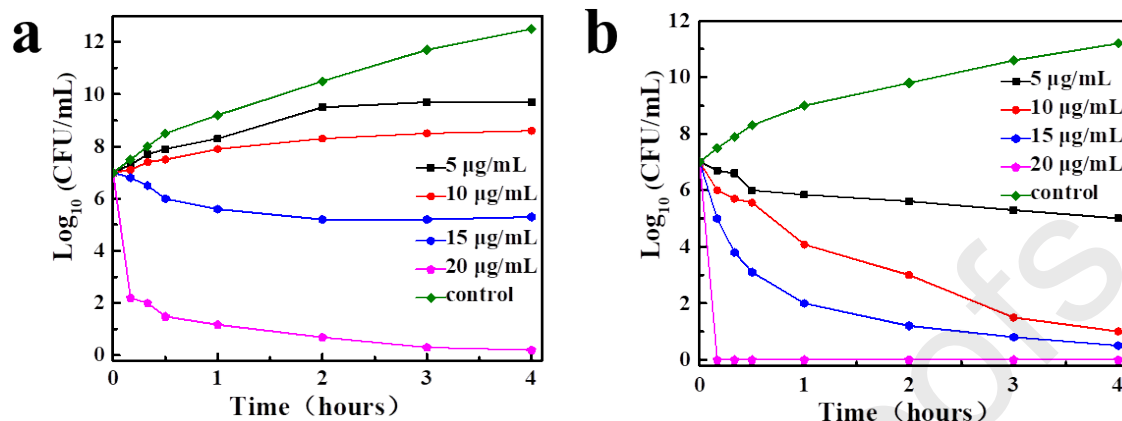


Fig. 3. Bactericidal kinetics of peptidomimetics against stationary phase *E. coli*: (a) A-L-Phe-C₁₂; (b) A-L-Val-C₁₂.

2.5. Biofilm disruption

Biofilm is an aggregate of bacteria held together by a mucus-like matrix of carbohydrate that adheres to a surface. This matrix is the basis for bacterial reproduction and spread. This bacterial community is an effective defense against antibiotics, making bacteria difficult to kill. Biofilm activity experiments were performed on biofilms formed by Gram-positive *S. aureus* and Gram-negative *E. coli* using peptidomimetic A-L-Val-C₁₂. The destructive activity of A-L-Val-C₁₂ against biofilm and bacteria in the biofilm was evaluated by measuring survival rate bacteria after peptidomimetic treatment.

Bacteria were statically incubated until a biofilm was formed, and A-L-Val-C₁₂ at different concentrations were used to treat the formed biofilm. As the concentration of A-L-Val-C₁₂ increased, the number of bacteria in the mature *E. coli* biofilm gradually decreased. At peptidomimetic concentrations greater than 16 $\mu\text{g/mL}$, the number of bacteria was significantly reduced to 13.7 log_{10} CFU. A further increase in peptidomimetic concentration to 256 $\mu\text{g/mL}$

reduced bacterial numbers to 2.5 log₁₀ CFU. As a control, the number of bacteria in untreated biofilm was 22.7 log₁₀ CFU per well—significantly higher than treated biofilm. A-L-Val-C₁₂ also showed bactericidal effects on bacteria in the *S. aureus* biofilm. At a peptidomimetic concentration of 256 µg/mL, the number of bacteria was 5.5 log₁₀ CFU; the number in untreated biofilm was 20.5 log₁₀ CFU per well. The above results indicate that peptidomimetic A-L-Val-C₁₂ can effectively destroy bacterial biofilm and kill embedded bacteria. A-L-Val-C₁₂ is more effective against the *E. coli* biofilm.

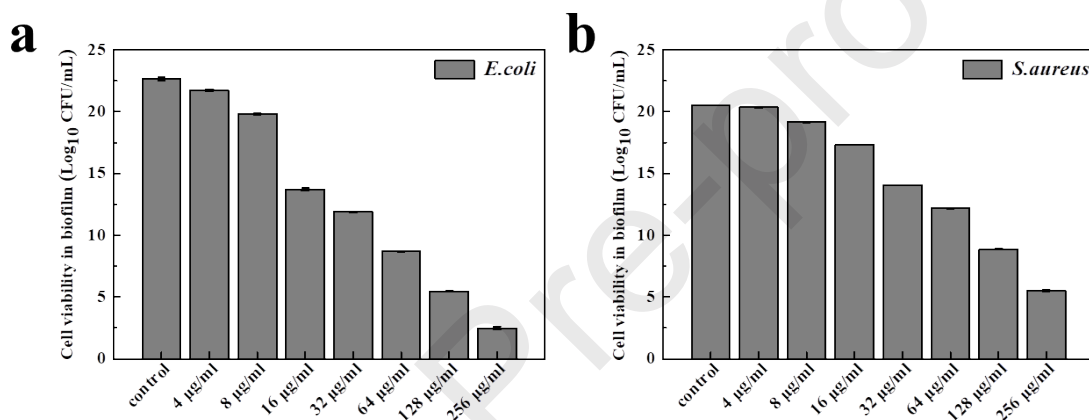


Fig. 4. Antibiofilm activity of A-L-Val-C₁₂ at different concentrations: (a) cell viability in non-treated and treated biofilms of *E. coli* grown on cover slips for 72 h; (b) cell viability in non-treated and treated biofilms of *S. aureus* grown on cover slips for 24 h.

2.6. Mechanism of action

Excellent and rapid bactericidal activity of peptidomimetics may be due to disruption of bacterial cell membrane integrity due to electrostatic interactions between negatively charged bacterial cell membrane with cationized peptidomimetics. Peptidomimetics, A-L-Phe-C₈, A-L-Phe-C₁₂, and A-L-Val-C₁₂, were separately incubated with Gram-negative *E. coli* and antibacterial mechanisms investigated using SEM, inverted fluorescence microscopy and flow cytometry (Fig. 5).

SEM images show that untreated *E. coli* shows a complete shape and a smooth surface, but *E. coli* treated with peptidomimetics exhibits obvious folds in the cell membrane, with some surface holes (Fig. 5a). Peptidomimetic treatment disrupts the cell membrane of bacteria, forming pores on its surface and leading to cell death.

The action of the peptidomimetics on bacterial cell membranes was investigated by the "live-dead staining" (N01 and PI) [34]. Staining of bacteria before and after the peptidomimetic treatment was observed using fluorescence microscopy. Untreated bacteria showed green and almost no red fluorescence, indicating normal *E. coli* cells and few or no dead bacteria. Only red fluorescence was observed for treated bacteria, indicating bacteria cell membrane rupture and cell death. Peptidomimetics effectively kill bacteria by destroying their cell membranes.

The cell proliferation was detected with Propidium Iodide (PI) single staining. After staining of DNA, DNA content of cells was measured by flow cytometry, and DNA replication and cell death were analyzed based on the distribution of DNA content. Except for the control group, fewer cells were viable. These results also indicate that peptidomimetics directly damage negatively charged cell membranes, leading to the leakage of genetic material and cell death.

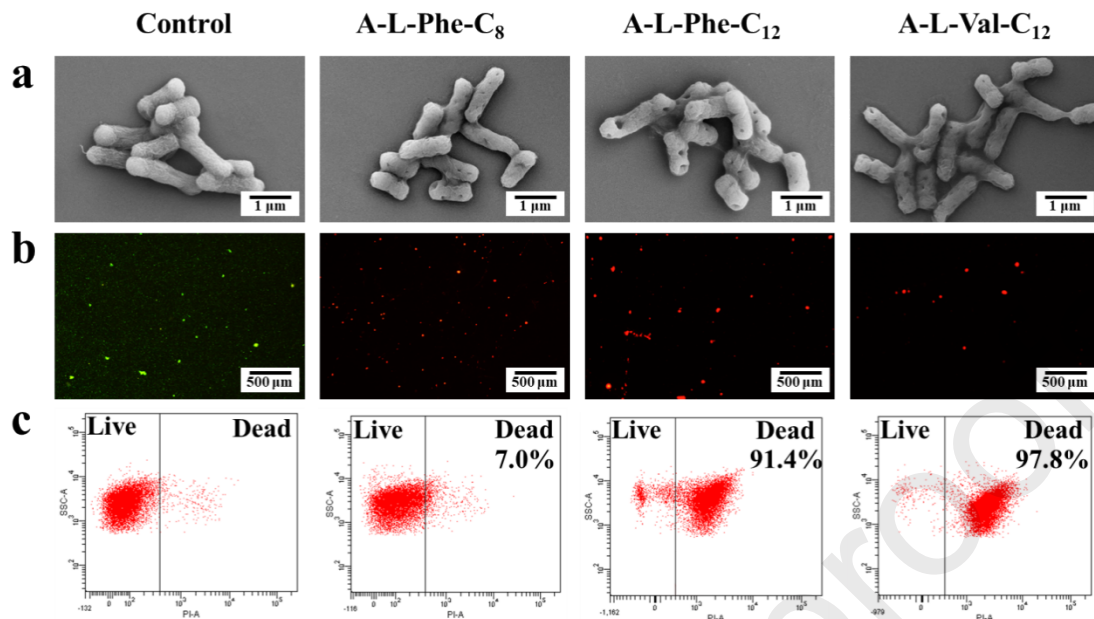


Fig. 5. Mechanism of antibacterial action before and after treatment with A-L-Phe-C₈, A-L-Phe-C₁₂ and A-L-Val-C₁₂ at same concentrations (10 μg/mL) against *E. coli*: (a) SEM images; (b) Fluorescence microscopy images after staining N01 and PI; (c) apoptotic rates measured by flow cytometry.

The antibacterial mechanism of the peptidomimetics is illustrated in Fig. 6. Cationic groups of peptidomimetics adsorbed to microbial surfaces through electrostatic interactions, thereby altering the electrochemical properties of the membrane surface. Further, due to the thin peptidoglycan layer between the inner and outer membranes of *E. coli* [35], long alkyl chains of the peptidomimetics more easily penetrate the cell membrane, resulting in perforation, leakage of intracellular material, and microbial cell death [36].

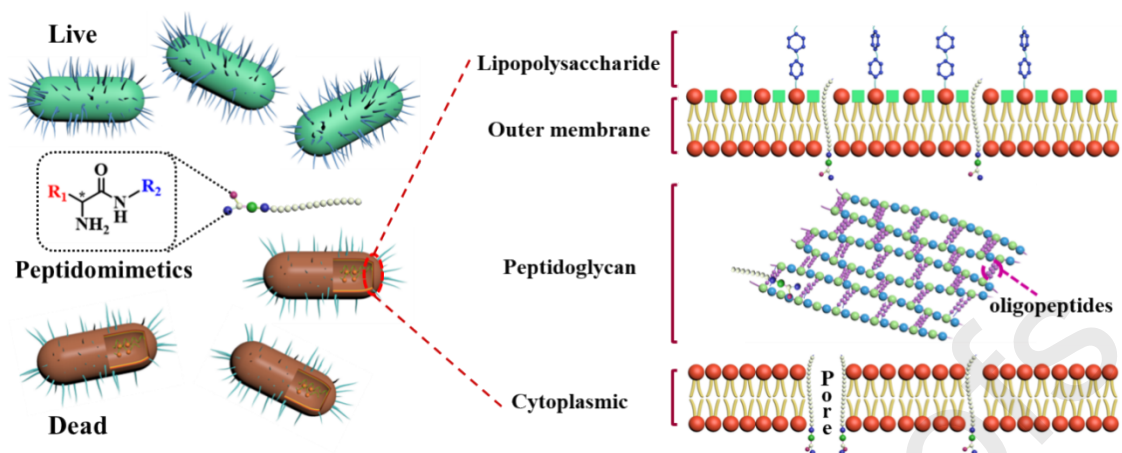


Fig. 6. The antibacterial mechanism of cationic peptidomimetics.

2.7. Antitumor cell activity

The excellent antibacterial and biofilm destruction activity of peptidomimetics, we investigated potential antitumor activity. Survival of SGC 7901 cells treated with three kinds of peptidomimetics (A-L-Phe-C₁₂, A-L-Val-C₁₂ and A-L-Phe-C₈) at different concentrations was investigated using the MTT approach (Fig. 7). Compared to controls, survival of SGC 7901 cells clearly decreased with increasing peptidomimetics concentration. Comparing the three peptidomimetics at the same concentration, survival of SGC 7901 cells treated with A-L-Phe-C₁₂ and A-L-Val-C₁₂ was less than the survival of the cells treated with A-L-Phe-C₈. A-L-Phe-C₁₂ and A-L-Val-C₁₂ are thus more potent for inhibiting SGC 7901 cells. Meanwhile, IC₅₀ values, concentrations needed for 50% cell growth inhibition estimated by curve fitting of absorbance values at different concentrations (Table 2). Peptidomimetics show promising anti-gastric cancer properties (IC₅₀=23-135 µg/mL) compatible with that of the reference, 5-Fluorouracil (IC₅₀=14 µg/mL).

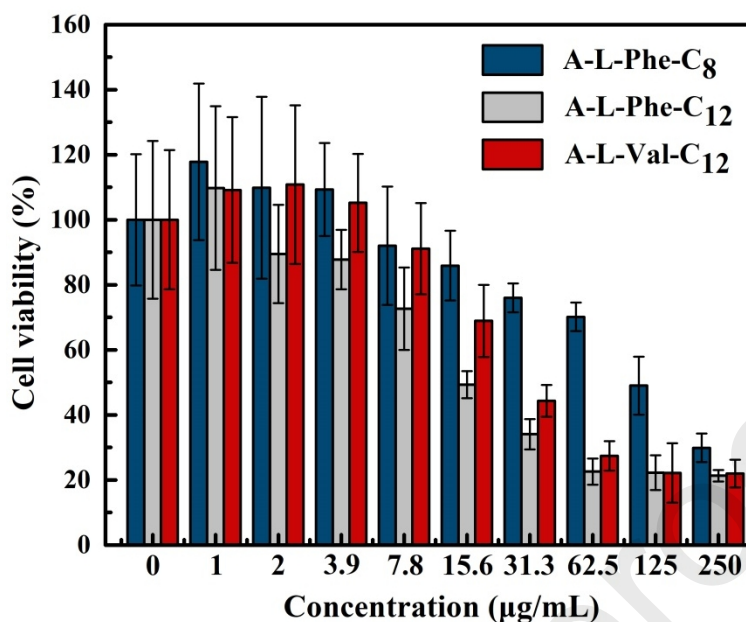


Fig. 7. The viability of SGC 7901 cells incubated with A-L-Phe-C₈ (blue), A-L-Phe-C₁₂ (gray) and A-L-Val-C₁₂ (red) at various concentrations.

Table 2. Antitumor properties of the tested peptidomimetics.

Peptidomimetic	A-L-Phe-C ₈	A-L-Phe-C ₁₂	A-L-Val-C ₁₂	5-Fluorouracil
IC ₅₀ (µg/mL)	135	23	37	14

Photographs from MTT assays indicate that cell membranes of control cells are structurally intact, but cells treated with peptidomimetic A-L-Val-C₁₂ are round or oval and show characteristics of apoptosis (Fig. 8a). Further, PI can cross damaged cell membranes and stain nuclei red, but cannot penetrate an intact cell membrane. The reagent is used to assess cell viability. PI staining was used to examine the effect of A-L-Val-C₁₂ on cell apoptosis. Except for the control group, cells in all the treated groups became more apoptotic in appearance (Fig. 8b). The percentage of apoptotic SGC 7901 cells treated with A-L-Val-C₁₂ was up to 56% at an A-L-Val-C₁₂ concentration of 30 µg/mL, much higher than 24.7% at 15 µg/mL and 11.1% at 7.5 µg/mL. These results indicate that A-L-Val-C₁₂ induces apoptosis in SGC 7901 cells, and the proportion

of apoptotic cells increased significantly with increasing concentration.

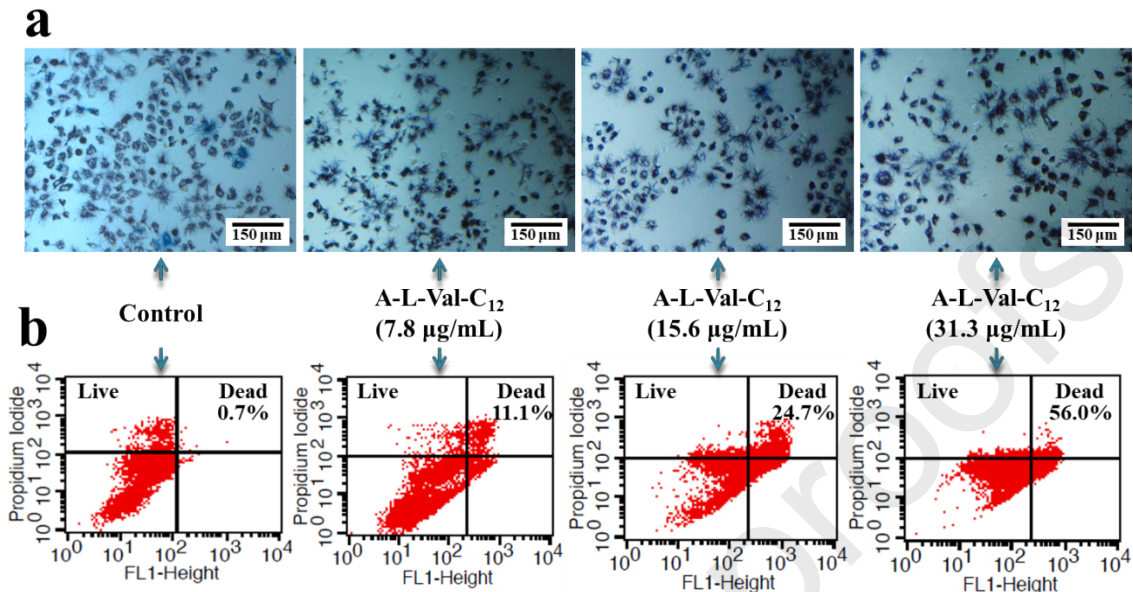


Fig. 8. Antitumor cell activity of A-L-Val-C₁₂: (a) morphology of the SGC 7901 cells; (b) apoptosis of SGC 7901 cells analyzed by flow cytometer.

2.8. Biocompatibility

Biocompatibility is an important topic in drug research, and cytotoxicity of the peptidomimetics was investigated by incubation of normal mammalian L929 cells with peptidomimetics A-L-Phe-C₈, A-L-Phe-C₁₂, and A-L-Val-C₁₂. All peptidomimetics show relatively low toxicity to L929 cells with a cell survival rate of more than 60%, even for a concentration of 1 mg/mL. Notably, at a concentration of 62.5 µg/mL, the survival rate of L929 cells incubated with the peptidomimetics was 100%. When a concentration of peptidomimetics is below 30 µg/mL, it exhibits good activity against gastric cancer SGC 7901 cells and significant antibacterial properties. Peptidomimetics are non-toxic to mammalian L929 cells at concentrations that can selectively act on gastric cancer cells SGC 7901 and bacteria. Thus, peptidomimetics display good biocompatibility.

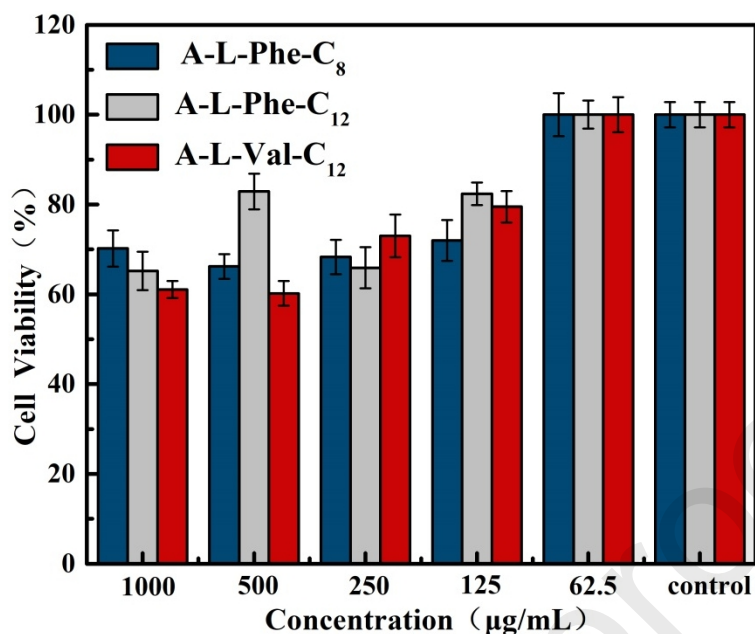


Fig. 9. Cell viability of L929 cells incubated with A-L-Phe-C₈ (blue), A-L-Phe-C₁₂ (gray) and A-L-Val-C₁₂ (red) at various concentrations.

3. Conclusions

A series of peptidomimetic antibacterial agents were successfully synthesized using amino acids as raw materials. The obtained peptidomimetics show excellent broad-spectrum antibacterial and biofilm destruction activity against both Gram-positive (including MRSA) and Gram-negative bacteria. These peptidomimetics are rapidly bactericidal via disrupting bacterial cell membranes and causing leakage of intracellular material. Further, peptidomimetics showed substantial inhibitory capacity on the growth of gastric cancer SGC 7901 cells, and low toxicity to mammalian normal L929 cells. These peptidomimetics have great potential to be developed as novel antibacterial and antineoplastic agents.

4. Experimental

4.1. Materials

Isobutyl chlorocarbonate, 3-aminophenylacetylene, L-phenylalanine, D-phenylalanine L-alanine, L-leucine, L-isoleucine, and L-phenylglycine were supplied by Saen Chemical Technology (Shanghai) Co., Ltd. 1-aminobutane, hexylamine, octylamine, decanamine, dodecylamine and hexadecylamine were purchased from Aladdin (China). Dichloromethane, Diethyl ether, Ethyl acetate, Triethylamine, Chloroform, Methanol, Hexane, NaOH, NaHCO₃, KHSO₄, anhydrous MgSO₄, beef, agar, PBS buffer and other solvents were supplied by Shanghai Macklin Biochemical Co., Ltd (China). The bacterial strains of *Staphylococcus aureus* (*S. aureus*) and *Bacillus subtilis*, Gram-negative *Escherichia coli* (*E. coli*) and *Salmonella enterica* and drug-resistant bacteria, methicillin-resistant *S. aureus* (MRSA) were provided by Shanghai Luwei Technology Co., Ltd. In this study, all reagents were analytical grade.

4.2. Measurements

¹H NMR (400MHz) spectra were recorded on a JEOL LEOLEX-400 spectrometer. The surface functional groups and chemical compositions of products were investigated using Fourier transform infrared spectroscopy (FT-IR, Nicolet Avatar-330) by the KBr pellet pressing method. The UV-vis absorption spectra were determined by a UV-1601 spectrophotometer. Bacterial growth was investigated using microplate reader (Mindray MR-96A). The morphological structures of the microorganisms were measured by scanning electron microscopy (SEM, Thermoscientific ApreoS LoVac, USA). Cells were observed under a DY5000X inverted microscope (Chongqing Photoelectric Instrument Co. Ltd., Chongqing, China). Cells and PI

single-stained cells for apoptosis were quantitatively assayed on a flow cytometer (Becton Dickinson, San Jose, CA, USA) using CellQuest software.

4.3. General procedure for the synthesis of amide coupling peptidomimetics

Various *N*-Boc protected amino acids were separately reacted with an aliphatic amine and with 3-aminophenylacetylene to produce the corresponding *N*-Boc protected peptidomimetics, and then removal of the Boc group provide the free peptidomimetics (Scheme 1). A typical procedure as follows: To a solution of *N*-Boc protected amino acids (10 mmol) in CH_2Cl_2 (20 mL) Et_3N (11 mmol) and isobutyl chloroformate (11 mmol) were added at 0 °C under stirring. After 55min, the amine (12.5 mmol) was added and the reaction was allowed to warm to room temperature and detected by TLC (hexane/ethyl acetate = 3:1, $R_f \approx 0.5$). After 24 h, the mixture was washed with 1M KHSO_4 , saturated NaHCO_3 , brine in sequence. The collected organic layer was dried over anhydrous MgSO_4 and then concentrated. The crude product was purified by flash column chromatograph to give the *N*-Boc protected peptidomimetics (35-78% yield).

Then, to a solution of *N*-boc protected peptidomimetics in ethyl acetate (8 mL) a solution of HCl in ethyl acetate (2 mL) was added and the mixture was stirred until the completion of the reaction (10 h). The ethyl acetate was evaporated and the mixture was washed with ether (3×20 mL). After concentration and dry in vacuum, the resulting compound was subsequently characterized by using ^1H NMR and ^{13}C NMR. (yield 55-90%)

4.3.1. (*S*)-2-Amino-*N*-butyl-3-phenylpropanamide (A-L-Phe-C₄)

White foamed solid, yield: 62.5%. ^1H NMR (400 MHz, DMSO-d_6) δ 8.50-8.37 (s, -CH-NH₂, 2H), 7.32-7.17 (m, Ar-H, 5H), 3.93 (dd, -NH-CO-CH-, 1H), 3.10–2.82 (m, -NH-CO-CH₂-, Ar-CH₂-, 4H), 1.36–0.95 (dt, -(CH₂)₂-CH₃, 4H), 0.80 (m, -CH₂-CH₃, 3H). ^{13}C NMR (101 MHz,

DMSO-d₆) δ 167.9, 135.6, 129.9, 128.8, 127.4, 53.9, 40.2, 38.7, 37.4, 31.2, 19.8, 14.1. IR (cm⁻¹,KBr) 3325(N-H), 1653(C=O), 1568(N-H).

4.3.2. (*S*)-2-Amino-*N*-hexyl-3-phenylpropanamide(A-L-Phe-C₆)

White foamed solid, yield: 57.2%. ¹H NMR (400 MHz, DMSO-d₆) δ 8.54-8.26 (s, -CH-NH₂, 2H), 7.31-7.10 (m, Ar-H, 5H), 3.93 (dd, -NH-CO-CH-, 1H), 3.10–2.82 (m, -NH-CO-CH₂-, Ar-CH₂-, 4H), 1.36–0.95 (dt, -(CH₂)₄-CH₃, 8H), 0.80 (m, -CH₂-CH₃, 3H). ¹³C NMR (101 MHz, DMSO-d₆) δ 167.9, 135.6, 129.9, 128.8, 127.4, 53.9, 39.9, 37.3, 31.4, 29.1, 26.4, 22.5, 14.4. IR (cm⁻¹,KBr) 3322(N-H), 1654(C=O), 1563(N-H).

4.3.3. (*S*)-2-Amino-*N*-octyl-3-phenylpropanamide(A-L-Phe-C₈)

White foamed solid, yield: 59.7%. ¹H NMR (400 MHz, DMSO-d₆): δ 8.55-8.15 (s, -CH-NH₂, 2H), 7.31-7.12 (m, Ar-H, 5H), 3.86 (dd, -NH-CO-CH-, 1H), 3.08–2.80 (dt, -NH-CO-CH₂-, Ar-CH₂-, 4H), 1.29–1.03 (dt, -(CH₂)₈-CH₃, 16H), 0.82 (m, -CH₂-CH₃, 3H). ¹³C NMR (101 MHz, DMSO-d₆) δ 167.9, 135.6, 130.1, 128.8, 127.4, 53.9, 40.1, 37.4, 31.7, 29.1, 26.7, 22.6, 14.4. IR (cm⁻¹,KBr) 3323(N-H), 1654(C=O), 1562(N-H).

4.3.4. (*S*)-2-Amino-*N*-decyl-3-phenylpropanamide(A-L-Phe-C₁₀)

White foamed solid, yield: 62.8%. ¹H NMR (400 MHz, DMSO-d₆) δ 8.48-8.25 (s, -CH-NH₂, 2H), 7.34-7.17 (m, Ar-H, 5H), 3.92 (dd, -NH-CO-CH-, 1H), 3.14–2.77 (dt, -NH-CO-CH₂-, Ar-CH₂-, 4H), 1.30–0.95 (dt, -(CH₂)₆-CH₃, 12H), 0.84 (m, -CH₂-CH₃, 3H). ¹³C NMR (101 MHz, DMSO-d₆) δ 167.9, 135.6, 129.9, 128.8, 127.4, 53.9, 39.9, 37.4, 31.8, 29.3, 26.7, 22.6, 14.4. IR (cm⁻¹,KBr) 3323(N-H), 1654(C=O), 1563(N-H).

4.3.5. (*S*)-2-Amino-*N*-dodecyl-3-phenylpropanamide(A-L-Phe-C₁₂)

White foamed solid, yield: 64.5%. ¹H NMR (400 MHz, DMSO-d₆) δ 8.48-8.28 (s, -CH-NH₂, 2H), 7.28-7.19 (m, Ar-H, 5H), 3.93 (dd, -NH-CO-CH-, 1H), 3.08–2.82 (dt, -NH-CO-CH₂-, Ar-CH₂-, 4H), 1.33–1.00 (dt, -(CH₂)₈-CH₃, 16H), 0.83 (m, -CH₂-CH₃, 3H). ¹³C NMR (101 MHz, DMSO-d₆) δ 168.0, 135.6, 129.9, 128.8, 127.4, 53.9, 40.1, 39.0, 37.4, 31.8, 29.5, 26.7, 22.6, 14.4. IR (cm⁻¹,KBr): 3323(N-H), 1654(C=O), 1563(N-H).

4.3.6. (*R*)-2-Amino-*N*-dodecyl-3-phenylpropanamide(A-D-Phe-C₁₂)

White foamed solid, yield: 59.7%. ¹H NMR (400 MHz, DMSO-d₆): δ 8.55-8.32 (s, -CH-NH₂, 2H), 7.31-7.18 (m, Ar-H, 5H), 3.94 (dd, -NH-CO-CH-, 1H), 3.08–2.80 (dt, -NH-CO-CH₂-, Ar-CH₂-, 4H), 1.29–1.03 (dt, -(CH₂)₈-CH₃, 16H), 0.82 (m, -CH₂-CH₃, 3H). ¹³C NMR (101 MHz, DMSO-d₆): δ 168.0, 135.8, 130.1, 128.9, 127.5, 54.1, 40.1, 37.5, 31.9, 29.5, 26.7, 22.6, 14.4. IR(cm⁻¹,KBr): 3323(N-H), 1654(C=O), 1563(N-H).

4.3.7. (*S*)-2-Amino-*N*-hexadecyl-3-phenylpropanamide(A-L-Phe-C₁₆)

White foamed solid, yield: 59.0%. ¹H NMR (400 MHz, DMSO-d₆): δ 8.39-8.28 (s, -CH-NH₂, 2H), 7.30-7.19 (m, Ar-H, 5H), 3.91 (dd, -NH-CO-CH-, 1H), 3.09–2.84 (dt, -NH-CO-CH₂-, Ar-CH₂-, 4H), 1.26–1.05 (dt, -(CH₂)₈-CH₃, 16H), 0.82 (m, -CH₂-CH₃, 3H). ¹³C NMR (101 MHz, DMSO-d₆): δ 167.9, 135.7, 130.1, 128.8, 127.4, 53.9, 40.1, 37.4, 31.8, 29.5, 26.8, 22.6, 14.4. IR(cm⁻¹,KBr): 3322(N-H), 1654(C=O), 1563(N-H).

4.3.8. (*S*)-2-Amino-*N*-dodecyl-3-methylbutanamide(A-L-Val-C₁₂)

Yellow viscous liquid, yield: 74.8%. ¹H NMR (400 MHz, DMSO-d₆): δ 7.73 (s, -CH-NH₂, 2H), 6.53 (s, -NH-CO-, 1H), 3.66 (s, -CH-NH₂, 1H), 3.06-2.93 (d, -CO-NH--CH₂-, 1H), 1.83 (s, -

(CH₃)₂-CH-CH₂-, 1H), 1.33,1.19 (s, -(CH₂)₁₀-CH₃, 20H), 0.78 (m, -CH₂-CH₃,-(CH₃)₂-CH-, 9H).
¹³C NMR (101 MHz, DMSO-d₆): δ 167.8, 57.8, 40.1, 31.8, 30.1, 29.5, 26.9, 22.6, 18.6, 14.3.
 IR(cm⁻¹,KBr): 3326(N-H), 1658(C=O), 1563(N-H).

4.3.9. (S)-2-Amino-N-dodecyl-4-methylpentanamide(A-L-Leu-C₁₂)

Dark orange viscous liquid, yield: 69.6%. ¹H NMR (400 MHz, DMSO-d₆): δ 8.63 (s, -NH-CO-, 1H), 8.29 (s, -CH-NH₂, 2H), 3.67 (s, -CH-NH₂, 1H), 3.15-2.94 (d, -CO-NH-CH₂-, 1H), 1.51 (m, -(CH₃)₂-CH-CH₂-, 1H), 1.20 (s, -CH-CH₂-CH-, -(CH₂)₁₀-CH₃, 22H), 0.81 (m, -CH₂-CH₃,-(CH₃)₂-CH-, 9H). ¹³C NMR (101 MHz, DMSO-d₆): δ 169.0, 71.7, 51.5, 39.8, 31.8, 29.3, 27.6, 26.7, 24.3, 22.7, 19.1, 14.4. IR(cm⁻¹,KBr): 3281(N-H), 1672(C=O), 1564(N-H).

4.3.10. (S)-2-Amino-N-dodecyl-3-methylpentanamide(A-L-Iso-C₁₂)

Dark green viscous liquid, yield: 70.6%. ¹H NMR (400 MHz, DMSO-d₆) δ 8.53 (s, -NH-CO-, 1H), 8.22 (s, -CH-NH₂, 2H), 3.69 (s, -CH-NH₂, 1H), 3.16,2.93 (d, -CO-NH-CH₂-, 1H), 1.77 (m, CH₃-CH-CH-, 1H), 1.49-1.35 (d, CH₃-CH₂-CH-), 1.20 (s, -(CH₂)₁₀-CH₃, 22H), 0.82 (m, -CH₂-CH₃, -CH-CH₃, 9H). ¹³C NMR (101 MHz, DMSO-d₆): δ 167.8, 65.4, 57.1, 39.8, 36.5, 31.8, 29.5, 26.8, 24.6, 22.6, 14.8, 14.3, 11.5. IR(cm⁻¹,KBr): 3281(N-H), 1672(C=O), 1564(N-H).

4.3.11. (S)-2-Amino-N-dodecyl-2-phenylacetamide(A-L-PG-C₁₂)

Dark yellow foamed solid, yield: 58.9%. ¹H NMR (400 MHz, DMSO-d₆): δ 7.44-7.02 (d, Ar-H, 5H), 3.18-2.78 (dt, -NH-CO-CH₂-, 2H), 1.33-1.00 (dt, -(CH₂)₁₀-CH₃, 20H), 0.83 (m, -CH₂-CH₃, 3H). ¹³C NMR (101 MHz, DMSO-d₆) δ 167.5, 135.0, 129.2, 128.1, 55.7, 40.1, 31.8, 29.5, 26.6, 22.6, 14.4. IR(cm⁻¹,KBr): 3324(N-H), 1657(C=O), 1561(N-H).

4.3.12. (*S*)-3-Amino-*N*-(3-ethynylphenyl)-5-methylhexanamide(A-L-Leu-mAA)

Dark yellow foamed solid, yield: 58.9%. ¹H NMR (400 MHz, DMSO-d₆): δ 8.00, 7.63 (dd, *Ar-H*, 4H), 4.21 (m, -NH-CO-*CH*-, 1H), 2.64 (s, Ph-C≡*CH*, 1H), 1.93-1.82 (m, (CH₃)₂-*CH*-), 1H), 1.81-1.08 (m, (CH₃)₂-*CH-CH*₂-), 2H), 0.89-0.79 (m, -(CH₃)₂-*CH*-, 6H). ¹³C NMR (101 MHz, DMSO-d₆) δ 197.1, 169.0, 143.0, 132.8, 129.9, 119.3, 52.2, 39.9, 27.0, 24.2, 23.1, 22.7. IR(cm⁻¹,KBr) 3287(N-H), 1694(C=O), 1553(N-H).

4.3.13. (*S*)-3-Amino-*N*-(3-ethynylphenyl)-4-methylhexanamide (A-L-Iso-mAA)

Dark green foamed solid, yield: 73.1%. ¹H NMR (400 MHz, DMSO-d₆): δ 7.87, 7.41 (m, *Ar-H*, 4H), 3.96 (m, -NH-CO-*CH*-, 1H), 2.52 (s, Ph-C≡*CH*, 1H), 2.07-1.70 (m, CH₃-*CH-CH*₂-), 1H), 1.89-1.25 (m, CH₃-*CH-CH*₂-), 2H), 1.02-0.76 (m, -*CH*₃-*CH*-, -*CH*₂-*CH*₃, 6H). ¹³C NMR (101 MHz, DMSO-d₆) δ 197.0, 168.0, 142.9, 132.8, 130.0, 119.3, 58.5, 39.9, 30.4, 27.0, 18.9, 18.3. IR(cm⁻¹,KBr) 3287(N-H), 1693(C=O), 1552(N-H).

4.4. Antibacterial tests

Determination of minimum inhibitory concentration (MIC)

MIC, the minimum concentration required for peptidomimetics to completely inhibit the bacterial growth. The antibacterial properties of the peptidomimetics against Gram-positive *S. aureus* and *Bacillus subtilis*, Gram-negative *E. coli* and *Salmonella enterica*, and a drug-resistant bacterium, methicillin-resistant *S. aureus* (MRSA) were assessed by the TTC coloration method [37]. The bacterial suspensions were incubated in the medium and diluted to the test concentration of 10⁷ CFU/mL. All the peptidomimetics were dissolved in sterile water and 0.02% TTC coloration agent prepared in liquid medium. TTC-containing liquid medium (100 μL) was added to each well

of the 96-well plate. Next, the peptidomimetics solutions (100 μL) were added to the 96-well plates and diluted in turn with three parallel experiments were conducted. Finally, the diluted bacterial suspensions (100 μL) were added to the 96-well plate. The mixtures were incubated at 37 $^{\circ}\text{C}$ (*Bacillus subtilis*) for 72 h or 37 $^{\circ}\text{C}$ (other bacteria) for 24 h. Negative contrast was a liquid culture containing 200 μL of media and a solution containing 200 μL of bacteria at 10^7 CFU/mL as a positive contrast. The MIC value is the lowest concentration without obvious bacterial growth. Therefore, due to the presence of TTC, the concentration of the peptidomimetics without red is MIC [37].

Inhibition Zone Test

The bacterial suspensions were incubated overnight at 37 $^{\circ}\text{C}$ in a freshly liquid medium. The diluted bacterial suspensions (10^7 CFU/mL, 100 μL) and agar medium were poured into a petri dish in sequence. The dish was shaken slightly before the solid medium solidifies to get homogeneous mixture of bacteria and solid medium. Finally, various peptidomimetics were placed in the Oxford cup on a solidified plate and incubated overnight at 37 $^{\circ}\text{C}$. After incubation, the inhibition zone around the Oxford cup was measured.

Biofilm disruption assay

S. aureus and *E. coli* were cultured for 4-6 h to attain the middle logarithmic stage. The bacterial suspensions ($\sim 10^5$ CFU/mL, 100 μL) were added to the 96-well plates, and the biofilm could be observed at the bottom of the plates for a certain period of time at 37 $^{\circ}\text{C}$ (*S. aureus* for 24 h, *E. coli* for 72 h). Then the 96-well plates were centrifuged at 3000 rpm for 5 min. The suspended liquid was removed and the wells were washed once with $1\times$ PBS. Sterile water was used to prepare A-L-Val-C₁₂ solutions with different concentrations. For the test group, the A-L-

Val-C₁₂ solutions (100 μ L) were added to the 96-well plates, while only 100 μ L of 1 \times PBS solution was added for the control group. After cultured at 37 $^{\circ}$ C for 24h, the supernatant was removed and the suspensions were centrifuged with 3000 rpm for 5min. The bacterial suspensions were diluted with a gradient of 10 times and dropped into the solid medium agar plate. After the culture of 24 h at 37 $^{\circ}$ C, colony counting was performed and the results were expressed by \log_{10} (CFU/well).

Bacterial growth inhibiting

E. coli from a single colony was inoculated into the liquid medium at 200 rpm and shaken overnight at 37 $^{\circ}$ C. Peptidomimetics with different concentrations and *E. coli* solution (OD₆₀₀ = 1, 200 μ L) were added to liquid medium (10 mL) in turn, and the final concentration range of the peptidomimetics was 1 μ g/mL to 20 μ g/mL. The liquid medium was incubated at 37 $^{\circ}$ C with 200 rpm. The bacterial suspensions without peptidomimetics were used as the blank control group. During incubation, the mixture (100 μ L) was poured into 96-well plates to measure the OD values of the bacterial suspensions at the wavelength of 600 nm. The growth inhibition curves of *E. coli* were obtained according to the OD values.

Bactericidal kinetics

In order to obtain the action rate of the peptidomimetics against bacteria, the bactericidal activity was evaluated by time killing kinetics test. The bacterial suspensions were diluted to concentration of 10^7 CFU/mL. Then, the peptidomimetics with the concentrations of 5 μ g/mL, 10 μ g/mL, 15 μ g/mL and 20 μ g/mL were added respectively. For comparison, a blank group without antibacterial agent was implemented. After dosing, each group was taken to 96-well plates and centrifuged at 3000rpm for 5min. The supernatant was removed, and 1 \times PBS solution (100 μ L) was suspended. The diluted bacteria (100 μ L) were dropped into the solid medium agar plate, and

the average value of each concentration was calculated. Then the agar plate was cultured overnight in a constant temperature incubator at 37 °C. The number of colonies was calculated in log (CFU/mL).

Fluorescence Microscopy

Peptidomimetics dissolved in sterile water were added to the *E.coli* suspensions (10^8 CFU/mL). The mixture was incubated for 1.5 h and washed with 0.85% NaCl at 9000 rpm for 5min. The mixture was dissolved in 0.85% NaCl (1 mL), then green fluorescent nucleic acid staining solution N01 (2 μ L) and red fluorescent nucleic acid staining solution PI (0.5 μ L) were added. The mixture was incubated at room temperature and out of light for 15 min and re-suspended with 0.85% NaCl to remove excess staining solution. The mixture (5 μ L) was dropped on the slide and examined with a fluorescence microscope.

Scanning Electron Microscopy (SEM)

The *E. coli* cells were cultured in liquid medium at 37 °C for 6 h. The cells were collected after centrifugation and re-suspended in liquid medium. Peptidomimetics with the concentration of 10 μ g/mL were added to the suspensions. The suspensions were incubated at 37 °C in a shaker for 2 h at 225 rpm, and the cells were collected by centrifugation at 9000 rpm. After treatment, the cells were fixed overnight with glutaraldehyde and then gradient dehydrated with 10 %, 30 %, 50 %, 70 %, 90 % and 100 % ethanol for 10 minutes. Dehydrated cells (5 μ L) were dropped to the silicon chip and dried at room temperature. The morphology of *E. coli* cells were observed by SEM.

4.5. Cell cytotoxicity and biocompatibility assay

MTT (3-(4, 5-dimethylthiazol-2-yl)-2, 5-diphenyl tetrazolium bromide) assay was used to appraise the toxicity of the peptidomimetics to L929 fibroblast cells and SGC 7901 cells. MTT method is a colorimetric and non-radioactive method to measure cell viability by increasing the metabolism of tetrazolium salt. The measurements were conducted in a 96-well opaque white plate with the L929 fibroblast cells and SGC 7901 cells density of about 7500 cells per well. After 24 h of culture with CO₂ (5 %, 37 °C), the cultured cells grew close to the culture bottle wall to form a monolayer. The cells were washed twice with serum-free medium (100 µL) and then starved for an hour at 37 °C. After starvation, cells were treated with different concentrations of the peptidomimetics for 24 h. At the end of the treatment, the as-prepared MTT stock solution (5 mg/mL, 0.02 mL) was added to each well and sequentially cultivated at 37 °C. The cells were washed with PBS (200 µL) to remove the redundant MTT containing medium. Then the crystals were dissolved in DMSO (100 µL) and the plate was shaken for 5 min at 125 rpm for the sake of solvent completely mixed with formazan which was obtained by reducing living cells metabolism determined by MTT. The optical density of formazan, which was directly proportional to the amount of living cells, was measured using a microplate reader regulated at 490 nm.

Then flow cytometry was used to detect apoptosis, and Annexin-V/FITC and PI were utilized to evaluate the apoptosis of SGC 7901 cells after different treatments of the peptidomimetics. The SGC 7901 cells were treated with different materials. After that, binding buffer (500 µL) and the staining of Annexin-V/FITC and PI (5 µL) were added to the mixture and the apoptosis was detected by the flow cytometry analyzer.

Acknowledgements

This work is financially supported by Natural Science Foundation of Heilongjiang Province, China (B2018003), the Fundamental Research Funds for the Central Universities (3072020CF1021). The authors are grateful for the support.

References

- [1] G.D. Wright, Molecular mechanisms of antibiotic resistance, *Chem. Commun.*, 47 (2011) 4055-4061.
- [2] M.H. Hannoun, M. Hagra, A. Kotb, A.-A.M.M. El-Attar, H.S. Abulkhair, Synthesis and antibacterial evaluation of a novel library of 2-(thiazol-5-yl)-1,3,4-oxadiazole derivatives against methicillin-resistant *Staphylococcus aureus* (MRSA), *Bioorg. Chem.*, 94 (2020).
- [3] K.K. Kumarasamy, M.A. Toleman, T.R. Walsh, J. Bagaria, F. Butt, R. Balakrishnan, U. Chaudhary, M. Doumith, C.G. Giske, S. Irfan, P. Krishnan, A.V. Kumar, S. Maharjan, S. Mushtaq, T. Noorie, D.L. Paterson, A. Pearson, C. Perry, R. Pike, B. Rao, U. Ray, J.B. Sarma, M. Sharma, E. Sheridan, M.A. Thirunarayan, J. Turton, S. Upadhyay, M. Warner, W. Welfare, D.M. Livermore, N. Woodford, Emergence of a new antibiotic resistance mechanism in India, Pakistan, and the UK: a molecular, biological, and epidemiological study, *Lancet Infect. Dis.*, 10 (2010) 597-602.
- [4] J. Monteiro, A.F. Santos, M.D. Asensi, G. Peirano, A.C. Gales, First Report of KPC-2-Producing *Klebsiella pneumoniae* Strains in Brazil, *Antimicrob. Agents Chemother.*, 53 (2009) 333-334.
- [5] M.L. McHenry, S.M. Williams, C.M. Stein, Genetics and evolution of tuberculosis pathogenesis: New perspectives and approaches, *Infect. Genet. Evol.*, 81 (2020) 9.

- [6] T.A. Wencewicz, Crossroads of Antibiotic Resistance and Biosynthesis, *J. Mol. Biol.*, 431 (2019) 3370-3399.
- [7] S.B. Levy, B. Marshall, Antibacterial resistance worldwide: causes, challenges and responses, *Nat. Med.*, 10 (2004) S122-S129.
- [8] C. Ghosh, J. Haldar, Membrane-Active Small Molecules: Designs Inspired by Antimicrobial Peptides, *ChemMedChem*, 10 (2015) 1606-1624.
- [9] V.J. Savage, I. Chopra, A.J. O'Neill, Staphylococcus aureus Biofilms Promote Horizontal Transfer of Antibiotic Resistance, *Antimicrob. Agents Chemother.*, 57 (2013) 1968-1970.
- [10] P.S. Stewart, J.W.J.L. Costerton, Antibiotic resistance of bacteria in biofilms, *Lancet*, 358 (2001) 135-138.
- [11] V. Yarlagadda, P. Akkapeddi, G.B. Manjunath, J. Haldar, Membrane Active Vancomycin Analogues: A Strategy to Combat Bacterial Resistance, *J. Med. Chem.*, 57 (2014) 4558-4568.
- [12] R.P. Dewangan, G.S. Bisht, V.P. Singh, M.S. Yar, S. Pasha, Design and synthesis of cell selective alpha/beta-diastereomeric peptidomimetic with potent in vivo antibacterial activity against methicillin resistant S. Aureus, *Bioorg. Chem.*, 76 (2018) 538-547.
- [13] D. Uppu, G.B. Manjunath, V. Yarlagadda, J.E. Kaviyil, R. Ravikumar, K. Paramanandham, B.R. Shome, J. Haldar, Membrane-Active Macromolecules Resensitize NDM-1 Gram-Negative Clinical Isolates to Tetracycline Antibiotics, *PLoS One*, 10 (2015).
- [14] B. Findlay, G.G. Zhanel, F. Schweizer, Cationic Amphiphiles, a New Generation of Antimicrobials Inspired by the Natural Antimicrobial Peptide Scaffold, *Antimicrob. Agents Chemother.*, 54 (2010) 4049-4058.
- [15] L.M. Yin, M.A. Edwards, J. Li, C.M. Yip, C.M. Deber, Roles of Hydrophobicity and Charge Distribution of Cationic Antimicrobial Peptides in Peptide-Membrane Interactions, *J. Biol. Chem.*,

287 (2012) 7738-7745.

[16] B.E. Haug, W. Stensen, M. Kalaaji, O. Rekdal, J.S. Svendsen, Synthetic antimicrobial peptidomimetics with therapeutic potential, *J. Med. Chem.*, 51 (2008) 4306-4314.

[17] M. Wu, E. Maier, R. Benz, R.E. Hancock, Mechanism of interaction of different classes of cationic antimicrobial peptides with planar bilayers and with the cytoplasmic membrane of *Escherichia coli*, *Biochemistry*, 38 (1999) 7235-7242.

[18] M.D. Seo, H.S. Won, J.H. Kim, T. Mishig-Ochir, B.J. Lee, Antimicrobial Peptides for Therapeutic Applications: A Review, *Molecules*, 17 (2012) 12276-12286.

[19] S.Q. Liu, S. Venkataraman, Z.Y. Ong, J.M.W. Chan, C. Yang, J.L. Hedrick, Y.Y. Yang, Overcoming Multidrug Resistance in Microbials Using Nanostructures Self-Assembled from Cationic Bent-Core Oligomers, *Small*, 10 (2014) 4130-4135.

[20] K. Kuroda, W.F. DeGrado, Amphiphilic polymethacrylate derivatives as antimicrobial agents, *J. Am. Chem. Soc.*, 127 (2005) 4128-4129.

[21] E.F. Palermo, S. Vemparala, K. Kuroda, Cationic Spacer Arm Design Strategy for Control of Antimicrobial Activity and Conformation of Amphiphilic Methacrylate Random Copolymers, *Biomacromolecules*, 13 (2012) 1632-1641.

[22] A. Hacker, L.J. Marton, M. Sobolewski, R.A. Casero, Jr., In vitro and in vivo effects of the conformationally restricted polyamine analogue CGC-11047 on small cell and non-small cell lung cancer cells, *Cancer Chemother. Pharmacol.*, 63 (2008) 45-53.

[23] Y.J. Zhang, T. Sun, C. Jiang, Biomacromolecules as carriers in drug delivery and tissue engineering, *Acta Pharm. Sin. B*, 8 (2018) 34-50.

[24] C. Oelkrug, M. Hartke, A. Schubert, Mode of Action of Anticancer Peptides (ACPs) from Amphibian Origin, *Anticancer Res.*, 35 (2015) 635-643.

- [25] M.V. Buri, T.M. Domingues, E.J. Paredes-Gamero, R.L. Casaes-Rodrigues, E.G. Rodrigues, A. Miranda, Resistance to Degradation and Cellular Distribution Are Important Features for the Antitumor Activity of Gomesin, *PLoS One*, 8 (2013).
- [26] D. Gaspar, A.S. Veiga, M.R.B. Castanho, From antimicrobial to anticancer peptides. A review, *Front Microbiol*, 4 (2013).
- [27] J. Hu, C.X. Chen, S.Z. Zhang, X.C. Zhao, H. Xu, X.B. Zhao, J.R. Lu, Designed Antimicrobial and Antitumor Peptides with High Selectivity, *Biomacromolecules*, 12 (2011) 3839-3843.
- [28] N. Papo, D. Seger, A. Makovitzki, V. Kalchenko, Z. Eshhar, H. Degani, Y. Shai, Inhibition of tumor growth and elimination of multiple metastases in human prostate and breast xenografts by systemic inoculation of a host defense-like lytic peptide, *Cancer Res.*, 66 (2006) 5371-5378.
- [29] C. Sinthuvanich, A.S. Veiga, K. Gupta, D. Gaspar, R. Blumenthal, J.P. Schneider, Anticancer beta-Hairpin Peptides: Membrane-Induced Folding Triggers Activity, *J. Am. Chem. Soc.*, 134 (2012) 6210-6217.
- [30] G. Sudhakar, S.R. Bathula, R. Banerjee, Development of new estradiol-cationic lipid hybrids: Ten-carbon twin chain cationic lipid is a more suitable partner for estradiol to elicit better anticancer activity, *Eur. J. Med. Chem.*, 86 (2014) 653-663.
- [31] M.M. Konai, J. Haldar, Lysine-Based Small Molecules That Disrupt Biofilms and Kill both Actively Growing Planktonic and Nondividing Stationary Phase Bacteria, *ACS Infect. Dis.*, 1 (2015) 469-478.
- [32] C. Ghosh, G.B. Manjunath, P. Akkapeddi, V. Yarlagadda, J. Hoque, D.S.S.M. Uppu, M.M. Konai, J. Haldar, Small Molecular Antibacterial Peptoid Mimics: The Simpler the Better!, *J. Med. Chem.*, 57 (2014) 1428-1436.
- [33] Y. Ge, D.L. MacDonald, K.J. Holroyd, C. Thornsberry, H. Wexler, M. Zasloff, *In vitro*

antibacterial properties of pexiganan, an analog of magainin, *Antimicrob. Agents Chemother.* 43 (4) (1999) 782-788.

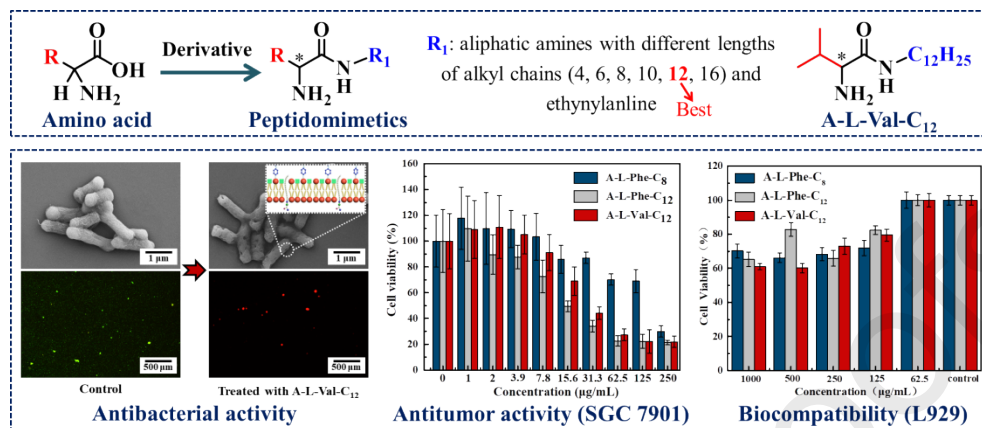
[34] K. Lienkamp, G.N. Tew, Synthetic Mimics of Antimicrobial Peptides-A Versatile Ring-Opening Metathesis Polymerization Based Platform for the Synthesis of Selective Antibacterial and Cell-Penetrating Polymers, *Chem. - Eur. J.*, 15 (2009) 11784-11800.

[35] A. Punia, A. Mancuso, P. Banerjee, N.-L. Yang, Nonhemolytic and Antibacterial Acrylic Copolymers with Hexamethyleneamine and Poly(ethylene glycol) Side Chains, *ACS Macro Lett.*, 4 (2015) 426-430.

[36] K. Lienkamp, K.-N. Kumar, A. Som, K. Nuesslein, G.N. Tew, "Doubly Selective" Antimicrobial Polymers: How Do They Differentiate between Bacteria?, *Chem. - Eur. J.*, 15 (2009) 11710-11714.

[37] A. Mourey, N. Canillac, Anti-*Listeria monocytogenes* activity of essential oils components of conifers, *Food Control*, 13 (2002) 289-292.

Graphical abstract



Highlights

- A series of peptidomimetics with alkyl or ethynyl phenyl substituents were synthesized from amino acids.
- The peptidomimetics exhibit broad-spectrum antibacterial properties, and the MIC for the tested strains including reached 2.5 ~ 4 $\mu\text{g} / \text{mL}$.
- The peptidomimetics have the potential to combat drug-resistant bacteria.
- The peptidomimetics showed good antitumor activity and low cytotoxicity.